Süleyman Demirel Üniversitesi Fen Edebiyat Fakültesi Fen Dergisi https://dergipark.org.tr/sdufeffd
Süleyman Demirel University Faculty of Arts and Sciences Journal of Science e-ISSN: 1306-7575
Research Article, 2024, 19(1): 75-85, DOI: 10.29233/sdufeffd.1364481

Investigating Thermal Neutron and Gamma Ray Shielding Properties of Al Matrix Gd_2O_3- and W-Doped Composites Using Monte Carlo Simulations

Yasin GAYLAN[1] and Ahmet BOZKURT[2]

[1]*Department of Medical Imaging Techniques, Zonguldak Bülent Ecevit University, 67100 Zonguldak, Turkey*
https://orcid.org/0000-0003-1354-7593
[2] *Department Of Computational Science And Engineering, Istanbul Tecnical University, 34469 Istanbul, Turkey*
https://orcid.org/0000-0002-3163-0131

(Received: 21.09.2023, Accepted: 16.04.2024, Published: 27.05.2024)

Abstract: This study aimed to calculate the thermal neutron (0.0253 eV) total macroscopic cross-section and gamma-ray (1.25 MeV) linear absorption coefficient for (100-x)Al-xGd_2O_3 (x=5 to 50) and 100-(x+y)Al-xGd_2O_3+yW (x,y=5 to 50) composites using MCNP6.2 simulation code. The simulation consists of a mono-energy point neutron and gamma-ray source, target material, and detector. The F4 tally from the MCNP6.2 library was used as the detector. The results show the highest thermal neutron total macroscopic cross-section for the 50%Al-50%Gd_2O_3 composite and the highest linear absorption coefficient for the 50%Al-%5Gd_2O_3-45%W composite. The results of this study provide a good understanding of the thermal neutron and gamma ray the shielding capabilities of Al matrix Gd_2O_3 and W doped composites.

Keywords: Al-Gd_2O_3-W composites, Neutron shielding, Gama shielding, Monte Carlo simulations

1. Introduction

Neutrons are used or emitted in nuclear power plants (during power generation and in fuel waste), particle accelerators, neutron imaging devices, elemental analysis and some biological applications [1–6]. Since neutrons have a net electric charge of zero, they do not enter into Coulomb interactions and interact with matter only at short distances (less than 1 fm) where the strong nuclear force is effective. For this reason, they can easily penetrate matter. Neutrons, depending on their energy, have a higher Relative Biological Effect and Radiation Weight Factor [7,8] compared to other types of ionizing radiation (p, α, γ, β-, β+). This makes neutron shielding a very important task when protecting workers and equipment in areas where neutron flux is present [9]. Neutron shields should be designed according to the restrictions and requirements of a specific usage [10–13]. Depending on their location/usage, neutron shielding properties, such as strength, portability, or heat resistance, become important [14].

Due to the high neutron absorption cross-section of the ^{10}B isotope, boron-containing materials have been widely studied to shield neutrons emitted during the storage and transport of spent fuel in dry storage casks or wet storage pools. Since B_4C cannot be formed into sheets due to its brittleness, it is produced as an aluminum-boron carbide (Al-B_4C) composite as a high-performance neutron shielding [15–18]. Studies show that the hardness as well as the neutron cross section of the Al-B_4C composite increases as the B_4C ratio increases and the machinability of the composite decreases. [19–23]. Therefore, literature studies suggest Al-30%B_4C composite as the ideal Al-B_4C composite ratio. [24,25]. In addition, the corrosion rate of neutron shielding increases

with increasing B_4C content in the composite as helium bubbles are generated due to the 10B(n, α) reaction. [26].

Therefore, rare earth elements with high neutron absorption cross-section, such as cadmium (Cd, 2520 barn), gadolinium (Gd, 49700 barn), samarium (Sm, 5922 barn), or europium (Eu, 4530 barn), have been utilized to enhance the absorption cross-section and ductility of Al-B_4C composites [27–29]. Among these elements, Gd has the highest thermal neutron absorption cross-section, so it has been widely studied to develop neutron shielding. Additionally, since Gd undergoes the (n, γ) reaction, it does not cause corrosion processes caused by the (n, α) reaction.

Xu et al. developed Al-(15%B_4C+1%Gd) composite as an alternative to Al-30%B_4C composite for shielding against thermal neutrons (0.0253 eV) [30]. They reported that reducing the B_4C ratio from 30% to 15% in the B_4C-Al composite and replacing it with 1%Gd increased its thermal neutron macroscopic cross-section from 24.9 cm^{-1} to 27.4 cm^{-1} and the elongation from 4% to 9%. Jiang et al. produced 6061Al-(1%Gd+15%B_4C) composite using vacuum hot pressing and hot rolling methods to enhance the ductility of spent fuel storage [31]. They reported that the mechanical properties of the composites were improved by the homogeneous distribution of Gd in the matrix. Moreover, the relationship between its fracture energy and the neutron total macroscopic cross-section exhibited a better performance than the B_4C/Al composites reported in the literature [22–24,32,33].

Since pure Gd is easily oxidized and very costly, Gd_2O_3 is an alternative. Zhang et al. obtained the neutron macroscopic cross-section of 6061Al-10%Gd_2O_3 and 6061Al-30%B_4C composites as Σ = 5.1 cm^{-1} and Σ=5.5 cm^{-1} respectively, in their study with neutrons of 0.2 eV energy. While the tensile strength values of both composites were equal (240 Mpa), the tensile strain increased from 4% in 6061Al-30%B_4C composite to 16% in 6061Al -10%Gd_2O_3 [34]. Cong et al. produced (100-x)%Al-x%Gd_2O_3 (x = 7, 15, 25, and 35) composites via powder metallurgy method with a cold isostatic press. The produced composites exhibited higher total macroscopic cross-section values for neutrons of 0.0253 eV energy than the Al-30%B_4C composite. Additionally, the thermal efficiency of the composite improved with increasing sintering time [35].

In order to absorb secondary gamma rays from the neutron absorption reaction, the neutron shielding is doped with elements with high gamma-ray linear attenuation coefficient. In comparison to lead (Pb) and bismuth (Bi) in neutron shielding [36], tungsten (W) stands out for gamma-ray absorption. In addition to its physical and mechanical properties, W is non-toxic, like Pb [37,38]. It also exhibits a higher thermal neutron absorption cross section (18.3 barn) than Pb (0.171 barn) [39].

Cong et al. examined Al-25%Gd_2O_3-x%W (x = 7, 15, 25 and 35) [40] composites as an alternative to Al-30%B_4C composite. They showed that Al-25%Gd_2O_3-25%W composite has a hardness value (88 HV) close to Al-30%B_4C composite, while thermal neutron and gamma-ray shielding properties are much better.

Researchers aiming to develop next-generation neutron shielding should address the following key questions when evaluating the Al-Gd_2O_3-W composite: whether its thermal neutron cross-section, gamma ray shielding properties (LAC, HVL, and TVL), and mechanical properties are

suitable.The composite with an optimal mixture ratio for these three properties is preferred as a suitable neutron shield. This study seeks to answer the first two questions to provide design concepts for Al-Gd_2O_3-W composites. In the simulation study, thermal neutron total macroscopic cross-section and LAC, HVL , TVL of 1.25 MeV gamma-rays were calculated for (100-x)Al-xGd_2O_3 (x=5 to 50) and 100-(x+y)Al-xGd_2O_3+yW (x,y=5 to 50) composites using the MCNP6.2 simulation code. This study is expected to guide the exploration of Al matrix Gd_2O_3- and W-doped composites, characterized by high strength and plasticity, by considering the thermal neutron cross-section and gamma-ray LAC, HVL and TVL values of Al-Gd_2O_3-W composition.

2. Materials and method

2.1 Monte Carlo simulations

This study used the Monte Carlo method to calculate the thermal neutron total macroscopic cross-section and gamma-ray shielding properties (LAC, HVL, and TVL). The radiation transport package MCNP6.2 simulation code is a Monte Carlo program that can simulate the transportation of neutrons, electrons, and photons through materials [41]. It was developed at Los Alamos National Laboratory for general-purpose radiation interactions. In the literature, MCNP has been used to calculate the radiation protection performance of various materials, such as concretes [42], glasses [43], and metal composites [33]. Simulation calculations for radiation shielding calculations are widely used in the literature [44–47].

As shown in Fig. 1, the simulation geometry consists of a mono-energetic point neutron/gamma-ray source placed in a cylindrical cavity, a target material in the form of a disk, and a cylindrical detector volume to measure the particle flux through the absorbing material. The thermal neutron energy is defined as $2.53*10^{-8}$ MeV, and the gamma-ray energy is defined as 1.25 MeV. The photon significance was set to zero (0) for thermal neutron total macroscopic cross-section calculations to shorten the simulation time. The detector flux was calculated using the F4 tally of MCNP6.2 simulation code, which measures the average flux in a cell per cm^2. To reduce statistical error, the simulations generated 10^8 histories (neutrons and gamma-rays) and the statistical error was below 1%.

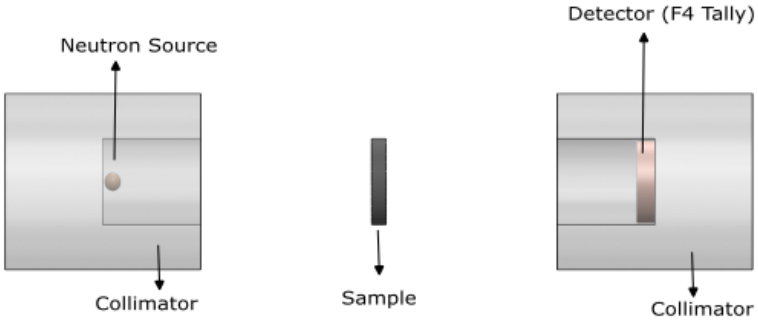

Figure 1. Geometrical setup for the monte carlo simulations

2.2 Calculation of total macroscopic cross-section (Σ_t) for neutrons

As neutrons pass through the matter, scattering or absorption reaction occurs, depending on their energy and the nucleus that makes up the matter. The neutron can perform nuclear fission, neutron capture, inelastic scattering, and elastic scattering reactions with the nucleus with which it interacts. The sum of the probability of neutron interacting with matter through the mentioned absorption σ_a and scattering σ_s reactions is defined as the total microscopic cross-section σ_t.

$$\sigma_t = \sigma_a + \sigma_s \quad (1)$$

When neutrons pass through a medium, the probability of scattering and absorption does not depend only on the microscopic scattering and absorption cross-section. The density of nuclei in the medium also affects the probability of the neutron passing through the medium and interacting. The microscopic cross-section and the density of nuclei in the medium are expressed by a physical quantity called the total macroscopic cross-section and is denoted by Σ_t [48];

$$\Sigma_t = N\sigma_t \quad (2)$$

N is the number of nuclei per unit volume, and the unit of Σ_t is cm^{-1}.

The total macroscopic cross-section of a material consisting of different nuclei is calculated as follows:

$$\Sigma_t = N_a\sigma_a + N_b\sigma_b + N_c\sigma_c + \cdots \quad (3)$$

The Σ_t value of a material is calculated using the Beer-Lambert law as follows [49];

$$I_x = I_0 e^{-\Sigma_t x} \quad (4)$$

Where x (in cm) is the thickness of the material, I_0 and I are the unattenuated and attenuated neutrons, and Σ_t (in cm^{-1}) is the total macroscopic cross-section.

2.3. Theoretical basis of gamma-ray shielding

When a gamma-ray beam passes through an absorbing medium, the intensity of the beam will be attenuated according to the Beer-Lambert law, so the linear absorption constant (μ) of the incident beam is calculated as follows;

$$I = I_0 e^{-\mu x} \quad (5)$$

Where x (in cm) is the thickness of the material, I_0 and I are the unattenuated and attenuated gamma-ray beam intensities, and μ (in cm^{-1}) are the linear attenuation coefficients.

Half Value Layer (HVL) is the thickness of a shield or an absorber that reduces the radiation level by a factor of 2 that is to half the initial level and is calculated by the following equation:

$$HVL = \frac{ln2}{\mu} = \frac{0,693}{\mu} \quad (6)$$

Similarly, the Tenth Value Layer (TVL) is defined as the thickness of a shield required for attenuating a radiation beam to 10% of its radiation level and is computed by,

$$TVL = \frac{ln10}{\mu} = \frac{2,3026}{\mu} \quad (7)$$

3. Results and Discussion

The thermal neutron total macroscopic cross-section values of (100-x)%Al-x%Gd_2O_3 (x=5 to 50) and 100(x+y)%Al-x%Gd_2O_3-y%W (x-y=5 to 50) composites are presented in Figure 2. As can be seen, the thermal neutron total macroscopic cross section increases with increasing Gd_2O_3 content in the composite. The thermal neutron total macroscopic cross-section value for the 95%Al-5%Gd_2O_3 composite is the lowest (22.7 cm^{-1}) among the Al-Gd_2O_3 series, while the value for the 50%Al-50%Gd_2O_3 composite is the highest (308.5 cm^{-1}). Compared to the reference Al-B_4C composite in the literature, the thermal neutron total macroscopic cross-section value of 26.68 cm^{-1} for the 70%Al-30%B_4C composite is lower than all Al-Gd_2O_3 composites in the series except the 95%Al-5%Gd_2O_3 composite.

In the Al-Gd_2O_3-W ternary composite, all composites except (95-x)%Al-5%Gd_2O_3-x%W (x=5, 10 and 15) composites have higher thermal neutron total macroscopic cross section values compared to the 70%Al-30%B_4C composite.

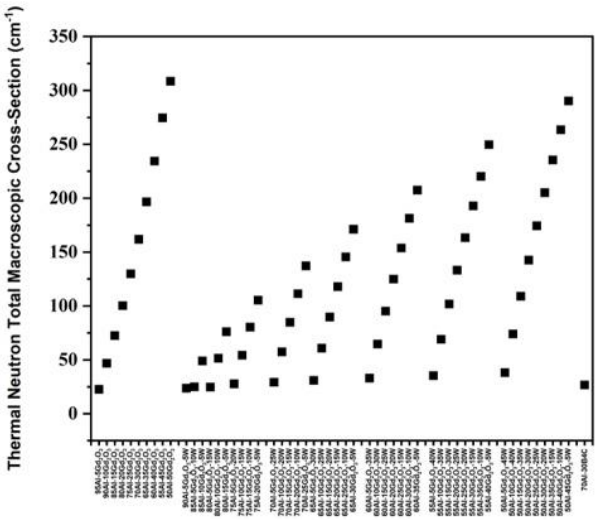

Figure 2. Thermal neutron total macroscopic cross-section of Al-Gd_2O_3/Al-Gd_2O_3-W composite combinations

The gamma-ray LAC, HVL, and TVL values of the (100-x)%Al-x%Gd_2O_3 (x=5 to 50) and 100-(x+y)%Al-x%Gd_2O_3-y%W (x-y=5 to 50) composites are depicted in Figure 3(a-c). As shown in Figure 3(a), the LAC of a composite increases when its Gd_2O_3 ratio increases. Among the Al-Gd_2O_3 series, 95%Al-5%Gd_2O_3 composite has the lowest gamma ray LAC value (0.154 cm^{-1}) and and the composite with the highest LAC value (0.213 cm^{-1}) is 50%Al-50%Gd_2O_3. In the case of the 100-(x+y)%Al-x%Gd_2O_3-y%W (x-y=5 to 50) composite, the LAC of a composite in the series decreases when its Gd_2O_3 ratio increases. The lowest LAC (0.161 cm^{-1}) is for the 90%Al-5%Gd_2O_3-5W composite, while the highest LAC (0.256 cm^{-1}) is for the 50%Al-5%Gd_2O_3-45%W composite. The LAC values of all Al-Gd_2O_3-W composites were calculated to be higher than that of the 70%Al-30%B_4C (0.144 cm^{-1}) composite. The LAC value of lead, accepted as a reference in gamma-ray absorption, was calculated as 0.656 cm^{-1}.

As shown in Figure 3(b-c), the highest HVL (3.19 cm) and TVL (10.6 cm) values were calculated for 50%Al-5%Gd_2O_3-45%W composite. Due to the high LAC value of tungsten, doping tungsten into the composite increases the gamma-ray shielding capability. In the literature, the HVL of lead used for gamma-ray shielding is calculated as 1.06 cm and the TVL as 3.51 cm.

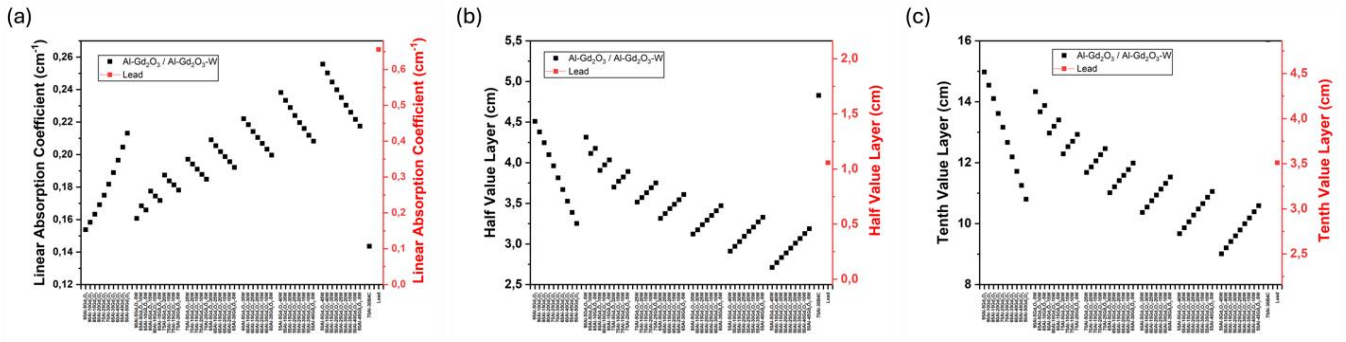

Figure 3. LAC, HVL, and TVL of Al-Gd_2O_3/Al-Gd_2O_3-W composite combinations

4. Conclusions

In this study, thermal neutron total macroscopic cross-section and gamma-ray LAC, HVL and TVL values of composites (100-x)%Al-x%Gd_2O_3 (where x=5 to 50) and 100-(x+y)%Al-x%Gd_2O_3-y%W (x-y=5 to 50) were calculated using the MCNP6.2 simulation code. This study investigated changes in the thermal neutron total macroscopic cross-sections and gamma-ray shielding properties of composites with Al matrix and Gd_2O_3 and W dopants. The results can be summarized as follows: The highest thermal neutron total macroscopic cross-section was calculated for the 50%Al-50%Gd_2O_3 composite. Gd is known to have the highest thermal neutron absorption cross-section. Therefore, doping Gd_2O_3 to the Al matrix significantly increases its thermal neutron total macroscopic cross-section. Similarly, Tungsten, with its high LAC value, increases the gamma-ray shielding properties of the composite when doped into the Al-Gd_2O_3 composite. The highest gamma-ray shielding value was calculated for the 50%Al-%5Gd_2O_3-45%W composite.

The cost of Gd_2O_3 is similar to that of B_4C and less than that of pure Gd. Since Gd has a much higher thermal neutron cross-section than B, adding only 5% Gd_2O_3 to the composite brings the thermal neutron total macroscopic cross-section closer to the value obtained with 30% B_4C doping.

Therefore, Gd_2O_3 is more cost-effective than B_4C. The composite formed with tungsten doping will be shielded in the secondary gamma-ray produced during the neutron absorption reaction.

Author contribution

Yasin GAYLAN: Investigation, Original Draft Writing, Review and Editing,

Ahmet BOZKURT: Review and Editing, Supervision

Conflicts of interest

There are no apparent conflicts.

Acknowledgments

N/A

Ethics Committee Approval and Informed Consent

As the authors of this study, we declare that we do not have any ethics committee approval and/or informed consent statement.

References

[1] E. G. Aydın, E. Tel, A. Kaplan, and A. Aydin, "Equilibrium and pre-equilibrium calculations of neutron production in medium-heavy targets irradiated by protons up to 100 MeV," Annals of Nuclear Energy, 35(12), 2306–2312, 2008.

[2] M. M. Castellanos, A. McAuley, and J. E. Curtis, "Investigating Structure and Dynamics of Proteins in Amorphous Phases Using Neutron Scattering," Computational and Structural Biotechnology Journal, 15, 117–130, 2017.

[3] A. Lombardi, D. Sediako, A. Machin, C. Ravindran, and R. MacKay, "Transient analysis of residual strain during heat treatment of multi-material engine blocks using in-situ neutron diffraction," Materials Letters, 157, 50–52, 2015.

[4] F. Mireles, J. I. Davila, J. L. Pinedo, E. Reyes, R. J. Speakman, and M. D. Glascock, "Assessing urban soil pollution in the cities of Zacatecas and Guadalupe, Mexico by instrumental neutron activation analysis," Microchemical Journal, 103, 158–164, 2012.

[5] T. Örs, F. Gouraud, R. Guinebretière, M. Huger, V. Michel, and O. Castelnau, "Neutron diffraction measurements of residual stress distribution in large zirconia based refractory bricks produced by electro-fusion and casting," Journal of the European Ceramic Society, 37(5), 2295–2302, 2017.

[6] T. Seymour, P. Frankel, L. Balogh, T. Ungár, S. P. Thompson, D. Jädernäs, J. Romero, L. Hallstadius, M. R. Daymond, G. Ribárik, and M. Preuss, "Evolution of dislocation structure in neutron irradiated Zircaloy-2 studied by synchrotron x-ray diffraction peak profile analysis," Acta Materialia, 126, 102–113, 2017.

[7] P. Schofield, B. Geiger, K. Sim, and A. J. Einstein, "ICRP Tahunan," 1–125, 2012.

[8] ICRP, "Annals of the International Commission on Radiological Protection, ICRP Publication 103," Ann. ICRP, 37(3–4), 332, 2007.

[9] R. C. Baumann and E. B. Smith, "Neutron-induced boron fission as a major source of soft errors in deep submicron SRAM devices," 2000 IEEE International Reliability Physics Symposium Proceedings, 152–157, 2000.

[10] S. Normand, B. Mouanda, S. Haan, and M. Louvel, "Discrimination methods between neutron and gamma rays for boron loaded plastic scintillators," Nuclear Instruments and Methods in Physics Research, Section A: Accelerators, Spectrometers, Detectors and Associated Equipment, 484(1–3), 342–350, 2002.

[11] M. Bastürk, J. Arztmann, W. Jerlich, N. Kardjilov, E. Lehmann, and M. Zawisky, "Analysis of neutron attenuation in boron-alloyed stainless steel with neutron radiography and JEN-3 gauge," Journal of Nuclear Materials, 341(2–3), 189–200, 2005.

[12] A. Nishimura, Y. Izumi, M. Imaizumi, S. Nishijima, T. Hemmi, and T. Shikama, "Neutron and gamma ray irradiation effects on interlaminar shear strength of insulation materials with cyanate ester-epoxy blended resin," Fusion Engineering and Design, 86(6–8), 1558–1561, 2011.

[13] Y. Tanabe, E. Yasuda, S. Kimura, T. Iseki, T. Maruyama, and T. Yano, "Neutron irradiation effects on dimension and mechanical properties of carbon fiber/carbon composite," Carbon, 29(7), 905–908, 1991.

[14] R. Lo Frano, G. Pugliese, and G. Forasassi, "Thermal analysis of a spent fuel cask in different transport conditions," Energy, 36(4), 2285–2293, 2011.

[15] F. Tang, X. Wu, S. Ge, J. Ye, H. Zhu, M. Hagiwara, and J. M. Schoenung, "Dry sliding friction and wear properties of B4C particulate-reinforced Al-5083 matrix composites," Wear, 264(7–8), 555–561, 2008.

[16] M. Alizadeh, "Strengthening mechanisms in particulate Al/B4C composites produced by repeated roll bonding process," Journal of Alloys and Compounds, 509(5), 2243–2247, 2011.

[17] M. Khakbiz and F. Akhlaghi, "Synthesis and structural characterization of Al-B4C nano-composite powders by mechanical alloying," Journal of Alloys and Compounds, 479(1–2), 334–341, 2009.

[18] A. Yazdani and E. Salahinejad, "Evolution of reinforcement distribution in Al-B4C composites during accumulative roll bonding," Materials and Design, 32(6), 3137–3142, 2011.

[19] K. Deng, J. Shi, C. Wang, X. Wang, Y. Wu, K. Nie, and K. Wu, "Composites : Part A Microstructure and strengthening mechanism of bimodal size particle reinforced magnesium matrix composite," Composites Part A, 43(8), 1280–1284, 2012.

[20] G. Luo, J. Wu, S. Xiong, Q. Shen, and C. Wu, "Microstructure and mechanical behavior of AA2024 / B 4 C composites with a network reinforcement architecture," Journal of Alloys and Compounds, 701, 554–561, 2017.

[21] I. Topcu, H. O. Gulsoy, N. Kadioglu, and A. N. Gulluoglu, "Processing and mechanical properties of B4C reinforced Al matrix composites," Journal of Alloys and Compounds, 482(1–2), 516–521, 2009.

[22] H. S. Chen, W. X. Wang, Y. L. Li, P. Zhang, H. H. Nie, and Q. C. Wu, "The design, microstructure and tensile properties of B4C particulate reinforced 6061Al neutron absorber composites," Journal of Alloys and Compounds, 632, 23–29, 2015.

[23] P. Zhang, Y. Li, W. Wang, Z. Gao, and B. Wang, "The design, fabrication and properties of B4C/Al neutron absorbers," Journal of Nuclear Materials, 437(1–3), 350–358, 2013.

[24] H. S. Chen, W. X. Wang, Y. L. Li, J. Zhou, H. H. Nie, and Q. C. Wu, "The design, microstructure and mechanical properties of B4C/6061Al neutron absorber composites fabricated by SPS," Materials and Design, 94, 360–367, 2016.

[25] Y. Gaylan, B. Avar, M. Panigrahi, B. Aygün, and A. Karabulut, "Effect of the B4C content on microstructure, microhardness, corrosion, and neutron shielding properties of Al–B4C composites," Ceramics International, 49(3), 5479–5488, 2023.

[26] F. Zhang, X. Wang, J. B. Wierschke, and L. Wang, "Helium bubble evolution in ion irradiated Al/B4C metal metrix composite," Scripta Materialia, 109, 28–33, 2015.

[27] R. G. Abrefah, R. B. M. Sogbadji, E. Ampomah-Amoako, S. A. Birikorang, H. C. Odoi, and B. J. B. Nyarko, "Comparison of the effects of cadmium-shielded and boron carbide-shielded irradiation channel of the Ghana Research Reactor-1," Nuclear Engineering and Design, 241(8), 3017–3020, 2011.

[28] S. Wan, W. Wang, H. Chen, J. Zhou, Y. Zhang, R. Liu, and R. Feng, "155/157Gd areal density: A model for design and fabrication of Gd2O3/316L novel neutron shielding composites," Vacuum, 176, 2020.

[29] R. Florez, H. A. Colorado, C. H. C. Giraldo, and A. Alajo, "Preparation and characterization of Portland cement pastes with Sm2O3 microparticle additions for neutron shielding applications," Construction and Building Materials, 191, 498–506, 2018.

[30] Z. G. Xu, L. T. Jiang, Q. Zhang, J. Qiao, D. Gong, and G. H. Wu, "The design of a novel neutron shielding B4C/Al composite containing Gd," Materials and Design, 111, 375–381, 2016.

[31] L. T. Jiang, Z. G. Xu, Y. K. Fei, Q. Zhang, J. Qiao, and G. H. Wu, "The design of novel neutron shielding (Gd+B4C)/6061Al composites and its properties after hot rolling," Composites Part B: Engineering, 168, 183–194, 2019.

[32] Y. Li, W. Wang, J. Zhou, H. Chen, and P. Zhang, "10B areal density: A novel approach for design and fabrication of B4C/6061Al neutron absorbing materials," Journal of Nuclear Materials, 487, 238–246, 2017.

[33] J. J. Park, S. M. Hong, M. K. Lee, C. K. Rhee, and W. H. Rhee, "Enhancement in the microstructure and neutron shielding efficiency of sandwich type of 6061Al-B4C composite material via hot isostatic pressing," Nuclear Engineering and Design, 282, 1–7, 2015.

[34] P. Zhang, J. Li, W. xian Wang, X. yue Tan, L. Xie, and F. yun Guo, "The design, microstructure and mechanical properties of a novel Gd2O3/6061Al neutron shielding composite," Vacuum, 162(January), 92–100, 2019.

[35] S. Cong, Y. Li, G. Ran, W. Zhou, and Q. Feng, "Microstructure and its effect on mechanical and thermal properties of Al-based Gd2O3 MMCs used as shielding materials in spent fuel storage," Ceramics International, 46(9), 12986–12995, 2020.

[36] K. Karimi-Shahri, L. Rafat-Motavalli, and H. Miri-Hakimabad, "Finding a suitable shield for mixed neutron and photon fields based on an Am-Be source," Journal of Radioanalytical and Nuclear Chemistry, 298(1), 33–39, 2013.

[37] H. Turkez, B. Cakmak, and K. Celik, "Evaluation of the Potential In Vivo Genotoxicity of Tungsten (VI) Oxide Nanopowder for Human Health," Key Engineering Materials, 543, 89–92, 2013.

[38] S. M. Hulbert and K. A. Carlson, "Is lead dust within nuclear medicine departments a hazard to pediatric patients?," Journal of Nuclear Medicine Technology, 37(3), 170–172, 2009.

[39] V. F. Sears, "Neutron News Neutron scattering lengths and cross sections," Neutron News, 1992.

[40] S. Cong, G. Ran, Y. Li, and Y. Chen, "Ball-milling properties and sintering behavior of Al-based Gd2O3–W shielding materials used in spent-fuel storage," Powder Technology, 369, 127–136, 2020.

[41] C. J. Werner, J. S. Bull, C. J. Solomon, F. B. Brown, G. W. McKinney, M. E. Rising, D. A. Dixon, R. L. Martz, H. G. Hughes, L. J. Cox, A. J. Zukaitis, J. C. Armstrong, R. A. Forster, and L. Casswell, "MCNP Version 6.2 Release Notes," 2018.

[42] M. I. Sayyed, K. A. Mahmoud, S. Islam, O. L. Tashlykov, E. Lacomme, and K. M. Kaky, "Application of the MCNP 5 code to simulate the shielding features of concrete samples with different aggregates," Radiation Physics and Chemistry, 174(March), 108925, 2020.

[43] R. El-Mallawany, M. I. Sayyed, M. G. Dong, and Y. S. Rammah, "Simulation of radiation shielding properties of glasses contain PbO," Radiation Physics and Chemistry, 151, 239–252, 2018.

[44] R. B. Malidarre, H. O. Tekin, Gunuglu Kadir, and H. Akyıldırım, "Assessment of Gamma Ray Shielding Properties for Skin," International Journal of Computational and Experimental Science and Engineering, 9(1), 6–10, 2023.

[45] B. Oruncak, "Computation of Neutron Coefficients for B2O3 reinforced Composite," International Journal of Computational and Experimental Science and Engineering, 9(2), 50–53, 2023.

[46] Z. Aygun and M. Aygun, "An Analysis on Radiation Protection Abilities of Different Colored Obsidians," International Journal of Computational and Experimental Science and Engineering, 9(2), 170–176, 2023.

[47] A. Coşkun, B. Cetin, İ. Yiğitoğlu, and H. Topakli, "Comparison of the Radiation Absorption Properties of PbO doped ZrB2 Glasses by using GATE-GEANT4 Monte Carlo Code and XCOM Programme," International Journal of Computational andExperimental Science and ENgineering (IJCESEN), 9(3), 274–279, 2023.

[48] J. E. Martin, *Physics for Radiation Protection, Third Edition* (Wiley-VCH, 2013).

[49] A. T. Boothroyd, *Principles of Neutron Scattering from Condensed Matter* (Oxford University Press, 2020).